

Universal Multilayer Network Exploration by Random Walk with Restart

Anthony Baptista^{a,b,1}, Aitor Gonzalez^b, and Anaïs Baudot^{a,d,1}

^aAix-Marseille Univ, INSERM, MMG, Turing Center for Living Systems, Marseille, France; ^bAix-Marseille Univ, INSERM, TAGC, Turing Center for Living Systems, Marseille, France; ^cBarcelona Supercomputing Center, Barcelona, Spain

This manuscript was compiled on July 12, 2021

The amount and variety of data is increasing drastically for several years. These data are often represented as networks, which are then explored with approaches arising from network theory. Recent years have witnessed the extension of network exploration methods to leverage more complex and richer network frameworks. Random walks, for instance, have been extended to explore multilayer networks. However, current random walk approaches are limited in the combination and heterogeneity of network layers they can handle. New analytical and numerical random walk methods are needed to cope with the increasing diversity and complexity of multilayer networks. We propose here MultiXrank, a Python package that enables Random Walk with Restart (RWR) on any kind of multilayer network with an optimized implementation. This package is supported by a universal mathematical formulation of the RWR. We evaluated MultiXrank with leave-one-out cross-validation and link prediction, and introduced protocols to measure the impact of the addition or removal of multilayer network data on prediction performances. We further measured the sensitivity of MultiXrank to input parameters by in-depth exploration of the parameter space. Finally, we illustrate the versatility of MultiXrank with different use-cases of unsupervised node prioritization and supervised classification in the context of human genetic diseases.

Multilayer Network | random walk | Data Integration

Data amount and variety have soared as never seen before. These data offer a unique opportunity to better understand complex systems. Among the different modes of representation of data, networks appear as particularly successful. Network representations are indeed particularly interesting to refine raw data and extract relevant features, patterns, and classes. They are exploited for years in the study of complex systems, and a wide and powerful range of tools from graph theory are available for their exploration.

However, the exploration and integration of large multidimensional datasets remains a major challenge in many scientific fields. For instance, a comprehensive understanding of biological systems would require the integrated analysis of dozens of different datasets produced at different molecular, cellular or tissular scales.

Recently, multilayer networks emerged as essential players of the analysis of complex systems. Multilayer networks allow integrating more than one network in a unified formalism, in which the different networks are considered as layers (1). For instance, Duran-Frigola et al. constructed a framework of 25 different networks of chemical compounds and their relationships (2), gathering relationships from chemical structures to clinical outcomes. These networks allow an integrated study of chemical compounds and their biological activities. Another example is given by the Hetionet project (3), in which the authors collected dozen of heterogeneous networks, i.e networks with various kinds of nodes such as genes, drugs or diseases to prioritize drugs for repurposing.

Several definitions of multilayer networks have been proposed based on the (in)homogeneity of the layers and the properties of the connections between layers (for review, see (4, 5)). For instance, multiplex networks are multilayer networks composed of different layers containing the same nodes

(called replica nodes) but different types of edges, and thereby different topologies. Heterogeneous networks link networks composed of different types of nodes thanks to bipartite interactions. Temporal networks follow the dynamic of a network over time: all the layers have the same nodes, but each layer represents the interaction state at a given time. We will here consider universal multilayer networks, which can be composed of any number of multiplex or monoplex networks (with edges that can be directed and/or weighted), linked by bipartite networks (with edges that can be directed and/or weighted) (Fig.1).

A wide range of methods has been developed in the recent years to analyze multilayer networks. For instance, different network metrics have been adapted to multilayer networks (6), as well as various network clustering algorithms for community detection (7–9) or random walk for network exploration (10–13).

Random walks are iterative stochastic processes widely used to explore network topologies. They can be described as simulated particles that walk iteratively from one node to one of its neighbors with some probability (14). The Pagerank algorithm, for instance, is based on a random walk process that simulates the behavior of an internet user walking from one page to another thanks to hyper-links. The user can also restart the walk on any arbitrary page (15). In this particular random walk strategy, the restart prevents the random walker from being trapped in dead-ends (16). An

A.Bap. and A.Bau. designed research; A.Bap. performed research; A.Bap. analyzed data; A.Bap. and A.G contributed to packaged code; A.Bap. and A.Bau. wrote the paper.

The authors declare no conflict of interest.

¹To whom correspondence should be addressed. E-mail: anthony.baptista@univ-amu.fr, anais.baudot@univ-amu.fr

arXiv:2107.04565v1 [cs.LG] 9 Jul 2021

interesting alternative strategy restricts the restart to specific node(s), called the seed(s) (17). In this random walk strategy, named Random Walk with Restart (RWR), the random walk represents a measure of proximity from all the nodes in the network to the seed(s). The RWR process can also be described as a diffusion process, in which the objective is to determine the steady-state of an initial probability distribution.

RWR are widely used to exploit large-scale networks. In computational biology, for instance, RWR strategies have been shown to significantly outperforms methods based on local distance measures for the prioritization of new gene-disease associations (18). Importantly, different upgrades of the RWR approach have been implemented during the last decade, including i) its extension to heterogeneous networks (10), ii) its extension to multiplex networks (11) and iii) its extension to multiplex-heterogeneous networks (13). In RWR, the degrees of freedom are summarized in the Transition rate matrix, and corresponds to the available transition between each node of the graph. The challenges of these different RWR extension lay in the normalization of the Transition rate matrices. To the best of our knowledge, this normalization is currently only solved for multilayer networks composed of two heterogeneous multiplex networks and the case of N multiplex networks remains unsolved.

We propose here MultiXrank, a new framework composed of a method and a Python package to execute RWR process on universal multilayer networks. We first introduce the mathematical bases of this universal RWR, which corresponds to a generalization of the approach from (10). We evaluated MultiXrank with leave one out cross-validation and link prediction protocols. These evaluations highlight in particular the critical influence of the bipartite networks. We then present an in-depth exploration of the parameter space to measure the stability of the RWR output scores under variations of the input parameters. We finally illustrate the versatility of MultiXrank with three different use-cases in the context of human genetic diseases: two unsupervised strategies for node prioritization and a supervised strategy to train a classifier. The MultiXrank Python package is freely available at <https://github.com/anthbapt/multixrank> with an optimized implementation allowing its application to large multilayer networks.

Universal Random Walk with Restart mathematical formulation

Random Walk with Restart (RWR).

Let us consider an irreducible Markov chain, for instance a network composed of a giant component with undirected edges, $G = (V, E)$. It is known in the case of irreducible Markov chains that a stationary probability p^* exists and satisfies the following properties:

$$\begin{cases} p_i^* \geq 0 ; & \forall i \in V \\ \sum_{i \in V} p_i^* = 1 \end{cases} \quad [1]$$

We introduce the probability that defines the walk from one node to another. Let define x , a particle that explores the

network, x_t its position at time t and x_{t+1} its position at time $t + 1$. Considering two nodes i and j :

$$\mathbb{P}(x_{t+1} = j, x_t = i) = \begin{cases} \frac{1}{d_i} & \text{if } (i, j) \in E \\ 0 & \text{Otherwise} \end{cases} \quad [2]$$

with d_i being the degree of the node i . All the normalized possible transitions can be included in the Transition rate matrix, noted M , which can be seen as the matrix of the degrees of freedom of the particle in the system. It is useful to note that the Transition rate matrix is here equal to the row-normalized Adjacency matrix. The distribution describing the probability of being in each node at time t is noted p_t , and the stationary distribution p^* is obtained thanks to the homogeneous linear difference equation [3] (16, 19):

$$p_{t+1}^T = M p_t^T \quad [3]$$

Moreover, we can introduce a non-homogeneous linear difference equation [4] (19), to take into account the restart on the seed(s). When the stationary distribution is reached (see supplementary section 1.A.1 for the proof of convergence), this distribution can be seen as a measure of proximity of all the network nodes to the seed(s).

$$p_{t+1}^T = (1 - r) M p_t^T + r p_0^T \quad [4]$$

The distribution p_0 corresponds to the initial probability distribution, where only the seed(s) have non-zero values, and r represents the restart probability.

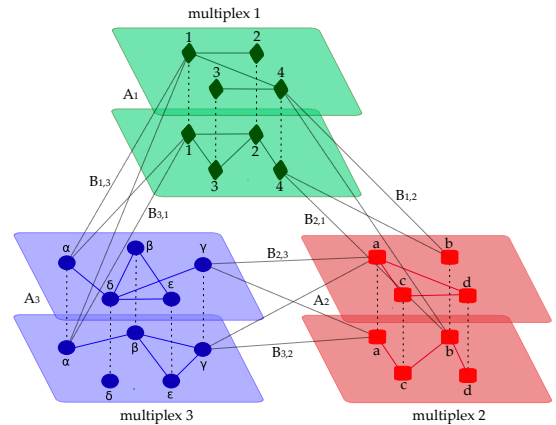


Fig. 1. A universal multilayer network composed of three multiplex networks (green, red and blue multiplex networks). Their corresponding Supra-adjacency matrices are noted A_i . The three Supra-adjacency matrices are linked by six bipartite networks (represented here as bipartite interactions for the sake of visualization). The corresponding Bipartite network matrices are noted $B_{i,j}$. Note that all the edges of the universal multilayer network can be weighted and/or directed.

RWR on Multiplex networks.

The RWR method was recently extended to multiplex networks (11, 12), i.e., multilayer networks with a one-to-one mapping between the (replica) nodes of the different layers (Fig.1) (1, 11). Multiplex networks can be represented by a Supra-adjacency matrix, which correspond to a generalization of the standard Adjacency matrix. For a multiplex network indexed by k , we note \mathcal{A}_k its Supra-adjacency matrix. Its dimension is equal to $(L_k * n_k) \times (L_k * n_k)$, with n_k the number of nodes by layers in the multiplex network k and L_k the number of layers in the multiplex network k . The Supra-adjacency matrix is defined as follows:

$$(\mathcal{A}_k)_{i\alpha, j\beta} = \begin{cases} (A_k^{[\alpha]})_{i,j} & \text{if } \alpha = \beta \\ \delta_{i,j} & \text{if } \alpha \neq \beta \end{cases} \quad [5]$$

where δ defines the Kronecker delta and α, β represent the layers of the multiplex network k . We can also define a multiplex network as a set of nodes, $V_{\mathcal{A}}$ and a set of edges, $E_{\mathcal{A}}$:

$$\begin{cases} G_{\mathcal{A}} = (V_{\mathcal{A}}, E_{\mathcal{A}}) \\ V_{\mathcal{A}} = \{v_i^\alpha, i = 1, \dots, n, \alpha = 1, \dots, L\} \\ E_{\mathcal{A}} = \{e_{i,j}^{\alpha\alpha}, i, j = 1, \dots, n, \alpha = 1, \dots, L, A_{i,j}^{[\alpha]} \neq 0\} \\ \quad \cup \{e_{i,i}^{\alpha\beta}, i = 1, \dots, n, \alpha \neq \beta\} \end{cases} \quad [6]$$

Importantly, we need to row-normalize the Supra-adjacency matrix defined in the equation [4] in order to converge to the steady-state, as defined in (13). This normalization requires including the parameters related to the jumps from one layer to another, i.e δ_k , inside the matrix representation, as described in (11) (Fig.2). In order to generalize the inclusion of the parameters related to the random walk with restart process to universal multilayer networks. As detailed in the next section, we need to index by k all the parameters that are dedicated to the multiplex network k . The Supra-adjacency matrix representing the multiplex network k can be written as described in equation [7]. The matrix $I_k \in \mathcal{M}_{n_k}(\mathbb{R})$ represents the Identity matrix.

$$\mathcal{A}_k = \begin{bmatrix} (1 - \delta_k)A_k^{[1]} & \frac{\delta_k}{(L_k - 1)}I_k & \dots & \frac{\delta_k}{(L_k - 1)}I_k \\ \frac{\delta_k}{(L_k - 1)}I_k & (1 - \delta_k)A_k^{[2]} & \dots & \frac{\delta_k}{(L_k - 1)}I_k \\ \dots & \dots & \dots & \dots \\ \frac{\delta_k}{(L_k - 1)}I_k & \frac{\delta_k}{(L_k - 1)}I_k & \dots & (1 - \delta_k)A_k^{[L_k]} \end{bmatrix} \quad [7]$$

RWR on universal multilayer networks.

We here define a new RWR method that can be applied to universal multilayer networks (Fig. 1). Universal multilayer networks are composed of any combination of multiplex networks, linked by any combination of bipartite networks. All networks can also be weighted and/or directed. The formalism for the application of RWR on multiplex networks is described in the previous section. We will now detail the Bipartite network matrices, and how to combine intra- and inter- multiplex networks information to obtain the Supra-heterogeneous adjacency matrix. The Supra-heterogeneous

adjacency matrix will embed all the possible transitions in a universal multilayer networks.

Bipartite networks connect heterogeneous information:

The Bipartite network matrices contain the transitions between the different types of nodes present in the different multiplex networks. Let us define \mathcal{A}_i and \mathcal{A}_j , two Supra-adjacency matrices representing the multiplex networks i and j . The Bipartite network matrix $B_{i,j}$ (resp. $B_{j,i}$) represents the transitions from the nodes of the multiplex network i (resp. j) to the nodes of the multiplex network j (resp. i). The size of the Bipartite network matrix $B_{i,j}$ (resp. $B_{j,i}$) is equal to $(L_i * n_i) \times (L_j * n_j)$ (resp. $(L_j * n_j) \times (L_i * n_i)$). The Bipartite network matrices are composed of $(n_i * n_j)$ duplications of the $b_{i,j}$ Bipartite network matrix, connecting all the layers of the multiplex network i with all the layers of the multiplex network j . We extended the formalism used in (13) in order to consider more than two different multiplex networks.

$$B_{i,j} = \underbrace{\begin{bmatrix} b_{i,j} & b_{i,j} & \dots & b_{i,j} \\ b_{i,j} & b_{i,j} & \dots & b_{i,j} \\ \dots & \dots & \dots & \dots \\ b_{i,j} & b_{i,j} & \dots & b_{i,j} \end{bmatrix}}_{n_j \text{ times}} \Bigg\} n_i \text{ times} \quad [8]$$

The representation of the bipartite networks as a set of nodes $V_{\mathcal{B}}$ and a set of edges $E_{\mathcal{B}}$ can be written as:

$$\begin{cases} G_{\mathcal{B}} = (V_{\mathcal{B}}, E_{\mathcal{B}}) \\ V_{\mathcal{B}} = \{v_k^i, k = 1, \dots, n_i\} \cup \{v_l^j, l = 1, \dots, n_j\} \\ E_{\mathcal{B}} = \{e_{k,l}^{ij}, k = 1, \dots, n_i, l = 1, \dots, n_j; (b_{i,j})_{k,l} \neq 0\} \end{cases} \quad [9]$$

It is to note that if the bipartite networks are undirected, $b_{j,i}^T = b_{i,j}$ and $B_{j,i}^T = B_{i,j}$

Universal multilayer networks unify the representation of heterogeneous multiplex networks:

We defined previously the Supra-adjacency matrices of each multiplex network and the Bipartite network matrices connecting the different multiplex networks. We now introduce the Supra-heterogeneous adjacency matrix, noted \mathcal{S} . This matrix, defined in equation [10], collects the N Supra-adjacency matrices representing each multiplex network, $\mathcal{A}_1, \mathcal{A}_2, \dots, \mathcal{A}_N$, and the $N(N-1)$ Bipartite network matrices connecting each multiplex network, $B_{1,2}, B_{1,3}, \dots, B_{1,N}, B_{2,1}, \dots, B_{N,N-1}$.

$$\mathcal{S} = \begin{bmatrix} \mathcal{A}_1 & B_{1,2} & \dots & B_{1,N} \\ B_{2,1} & \mathcal{A}_2 & \dots & B_{2,N} \\ \dots & \dots & \dots & \dots \\ B_{N,1} & B_{N,2} & \dots & \mathcal{A}_N \end{bmatrix} \quad [10]$$

We can also define the Supra-heterogeneous adjacency matrix as a set of nodes and edges:

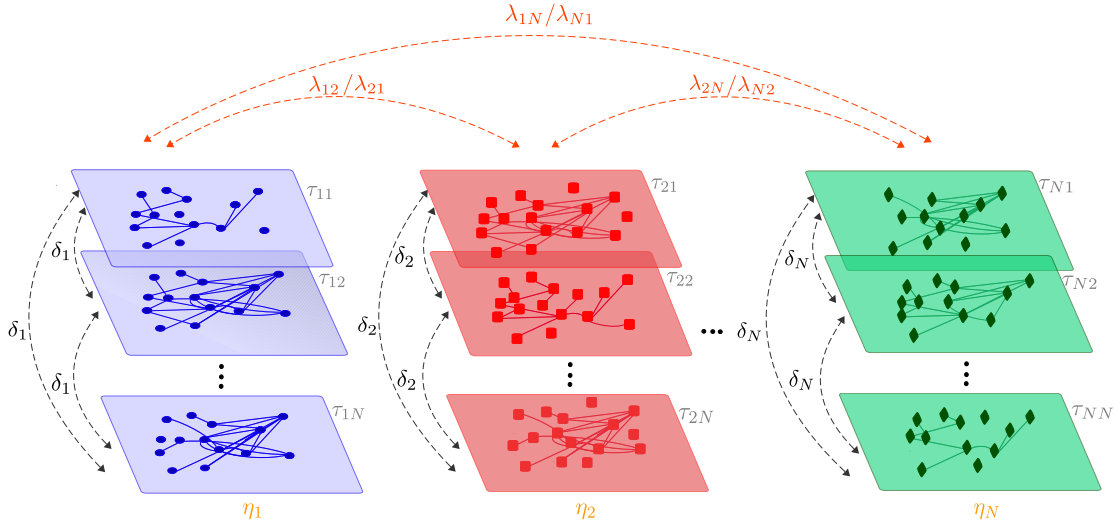


Fig. 2. MultiXrank RWR parameters to explore universal multilayer networks composed of N multiplex networks (each composed of several layers containing the same set of nodes but different edges). The parameters δ are associated with the probability to jump from one layer to another in a given multiplex network, λ with the probability to jump from one multiplex network to another multiplex network, τ with the probability to restart in a given layer of a given multiplex network, and η with the probability to restart in a given multiplex network.

$$\left\{ \begin{array}{l} G_S = (V_S, E_S) \\ V_S = \bigcup_{k=1}^N \{v_{k,i}^{\alpha_k}, i = 1, \dots, n_k, \alpha_k = 1, \dots, L_k\} \\ E_S = \bigcup_{k=1}^N \{ \{e_{i,j}^{\alpha_k, \alpha_k}, i, j = 1, \dots, n_k, (A_k)_{i,j}^{[\alpha_k]} \neq 0\} \\ \cup \{e_{i,i}^{\alpha_k, \beta_k}, i = 1, \dots, n_k, \alpha_k \neq \beta_k\} \} \\ \cup \bigcup_{k,l=1; k \neq l}^N \{e_{i,j}^{\alpha_k, \alpha_l}, i = 1, \dots, n_k, j = 1, \dots, n_l, (B_{k,l})_{i,j} \neq 0\} \end{array} \right. \quad \widehat{S}_{\alpha\alpha}(i_\alpha, j_\alpha) = \begin{cases} \frac{A_\alpha(i_\alpha, j_\alpha)}{\sum_{k_\alpha=1}^{n_\alpha} A_\alpha(i_\alpha, k_\alpha)} & \text{if } \forall \beta : \sum_{k_\beta=1}^{n_\beta} B_{\alpha,\beta}(i_\alpha, k_\beta) = 0 \\ \frac{(1 - \sum_{\beta=1}^c \lambda_{\alpha\beta}) * \lambda_{\alpha\alpha} A_\alpha(i_\alpha, j_\alpha)}{\sum_{k_\alpha=1}^{n_\alpha} A_\alpha(i_\alpha, k_\alpha)} & \text{Otherwise} \end{cases} \quad [13]$$

The normalization of the Supra-heterogeneous adjacency matrix ensures the convergence of the RWR to the steady-state: The most complex issue is the normalization of the Supra-heterogeneous adjacency matrix into a Transition rate matrix that can be used in equation [4]. The normalization allows obtaining a Stochastic matrix that guarantees the convergence of the RWR to the steady-state (see proof in supplementary section 1.A.1). It is important to note that we have chosen a row normalization. The resulting normalized matrix, noted \widehat{S} is defined in equation [12]. We generalized the formalism of (10), established for two heterogeneous monoplex networks, to universal multilayer networks, thanks to intra- and inter- multiplex networks normalization defined in equations [13-14], with $\alpha \in [1, N]$, $\beta \in [1, N]$, and c the number of bipartite networks where the node i_α appears as source multiplex network α , noted M_α .

$$\widehat{S} = \begin{bmatrix} \widehat{S}_{11} & \widehat{S}_{12} & \dots & \widehat{S}_{1N} \\ \widehat{S}_{21} & \widehat{S}_{22} & \dots & \widehat{S}_{2N} \\ \dots & \dots & \dots & \dots \\ \widehat{S}_{N2} & \widehat{S}_{N2} & \dots & \widehat{S}_{NN} \end{bmatrix} \quad [12]$$

$$\widehat{S}_{\alpha\beta}(i_\alpha, j_\beta) = \begin{cases} \frac{\lambda_{\alpha\beta} B_{\alpha,\beta}(i_\alpha, j_\beta)}{\sum_{k_\beta=1}^{n_\beta} B_{\alpha,\beta}(i_\alpha, k_\beta)} & \text{if } \sum_{k_\beta=1}^{n_\beta} B_{\alpha,\beta}(i_\alpha, k_\beta) \neq 0 \\ \frac{\lambda_{\alpha\beta}}{\sum_{i_\alpha=1}^c \lambda_{\alpha\beta} \sum_{i_\alpha=1}^c B_{\alpha,\beta}(i_\alpha, j_\beta)} & \text{if } i_\alpha \text{ not in } M_\alpha \\ 0 & \text{Otherwise} \end{cases} \quad [14]$$

The normalization allows including the parameters λ_{ij} to jump between the different multiplex networks (Fig. 2). In other words, these parameters weight the jumps from one multiplex network i to another multiplex network j , if the bipartite interaction exists. Moreover, the standard probability condition of normalization imposes that $\sum_{i=1}^N \lambda_{ij} = 1, \forall j$, with N the number of multiplex networks. Finally, the universal RWR equation is defined as:

$$p_{t+1}^T = (1 - r) \widehat{S} p_t^T + r p_0^T \quad [15]$$

RWR initial probability distribution in universal multilayer networks: The initial probability distribution p_0 from equation [15], which contains the probabilities to restart on the seed(s), can be written in its general form as follows:

$$p_0^T = \begin{bmatrix} \eta_1 \bar{\mathbf{v}}_0^1 \\ \eta_2 \bar{\mathbf{v}}_0^2 \\ \dots \\ \eta_N \bar{\mathbf{v}}_0^N \end{bmatrix} \quad [16]$$

with η_k the probability to restart in one of the layers of the multiplex network k , and $\bar{\mathbf{v}}_0^k$ the initial probability distribution of the multiplex network k . The size of $\bar{\mathbf{v}}_0^k$ is equal to $(L_k * n_k)$ with L_k the number of layers in the multiplex network k and n_k the number of nodes in the multiplex network k . We constraint the parameter η with the standard probability condition of normalization that imposes $\sum_{i=1}^N \eta_i = 1$. We defined another parameter τ to take into account the probability of restarting in the different layers of a given multiplex network. This parameter include τ_{ij} , where i corresponds to the index of the multiplex network (i) and j to the index of the layer of the multiplex network (i) (Fig.2). In other words, τ_{ij} corresponds to the probability to restart in the j^{th} layer of the multiplex network i . Finally, $\bar{\mathbf{v}}_0^k$ is defined as follows: $\bar{\mathbf{v}}_0^k = [\tau_{i1} v_0^k, \tau_{i2} v_0^k, \dots, \tau_{in_i} v_0^k]^T$, with v_0^k being a vector with ones in the position(s) of seed(s) and zeros elsewhere. The probability condition of normalization gives the constraint: $\sum_{j=1}^{L_k} \tau_{ij} = 1, \forall i$.

Numerical implementation: MultiXrank.

Our RWR on universal multilayer networks method is implemented as a Python package called MultiXrank with an optimized implementation. Default parameters allow exploring homogeneously the multilayer network (supplementary section 1.B). The running time of the package depends on the number of edges of the multilayer network (see complexity analyses in supplementary section 2.A).

The package is available on GitHub [github/MultiXrank](https://github.com/MultiXrank), and can be installed with standard pip installation command: [pypi/MultiXrank](https://pypi.org/project/MultiXrank).

Evaluations and Parameter space exploration

Evaluations.

We first evaluated the performance of MultiXrank using two different multilayer networks. The first one is a large biological multilayer network composed of a gene multiplex network gathering gene physical and functional relationships, a disease monoplex network representing disease phenotypic similarities, and a drug multiplex network containing drug clinical and chemical relationships. Each monoplex/multiplex network is connected to the others thanks to bipartite networks containing gene-disease, drug-gene, and drug-disease interactions (supplementary section 3.B). The second multilayer network is composed of three multiplex networks: a French airports multiplex network, a British airports multiplex network, and a German airports multiplex network. In each multiplex network, the nodes represent the airports and the edges the national flight connections between these airports for three airline companies. These three multiplex networks are linked with bipartite networks corresponding to transnational flight connections (supplementary section 3.A).

We designed a Leave-One-Out Cross-Validation (LOOCV) protocol inspired by F.Mordelet and J.P.Vert (20) and

A.Valdeolivas et al. (13). The protocol assesses the reconstruction of left-out data using the data remaining in the network. In the case of the biological multilayer network, we left-out data from the gene-disease bipartite network: the edges associating genes with a given disease are removed one by one. Each time a gene-disease edge is removed, the corresponding gene is considered as the left-out gene. The remaining genes associated with the same disease are used as seed(s), together with the disease node when the disease network is considered in the RWR. We considered only diseases associated with at least two genes. The RWR algorithm is then applied, and all the network nodes are scored according to their proximity to the seed(s). The rank of the gene node that was left-out in the ongoing run is recorded. The gene left-out process is repeated iteratively. Finally, the Cumulative Distribution Function (CDF) of the ranks of the left-out genes is plotted (Fig. 3). The CDF displays the percentage of left-out genes that are ranked by the RWR within the top-K ranked gene nodes. The CDFs are used to evaluate and compare the performance of the RWR using different combinations of biological networks: the protein-protein interactions (PPI) network, the gene multiplex network, the multilayer network composed of the gene multiplex and disease monoplex networks, and the multilayer network composed of the gene multiplex, disease monoplex, and drug multiplex networks (Fig. 3 panel A.1).

We observed that considering multiple sources of network data is always better than considering the PPI alone. In addition, considering multilayer information is better than considering only the gene multiplex network. However, the increased performances in the LOOCV seems to arise only from the consideration of the gene multiplex network with the disease monoplex network (and associated gene-disease bipartite network). Indeed, the addition of the drug multiplex network (and associated drug-gene and drug-disease bipartite networks) to the system does not increase the performances (Fig. 3 panel A.1).

We repeated the same LOOCV protocol for the airports multilayer network, in which the left-out nodes are French airport nodes associated with a given British airport node. Here, the behavior is different, as adding the multiplex network of German airports connections (and associated French-German and British-German bipartite networks) increases the performances of the RWR to predict the associations between French and British airports (Fig. 3 panel A.2).

To better understand these behaviors, we examined in detail the overlaps between the different bipartite networks. We observed that only 23% of the genes from the gene-disease bipartite network are present in the drug-gene bipartite network. Similarly, only 5% of the diseases from the gene-disease bipartite network are present in the disease-drug bipartite network (Fig. S10). Given this low overlaps, the drug multiplex network might not contribute significantly to connecting gene and disease nodes during the random walks, which might explain why adding the drug multiplex network does not improve the performances of the LOOCV. Contrarily, the airport multilayer network displays high overlaps between the different bipartite networks (Fig. S10), which might explain why the addition of the third multiplex network in this case increases the predictive power (Fig.3 panel A.2).

To validate the proposed central role of bipartite network overlaps in the RWR performances, we artificially increased

the connectivity of the gene-drug and disease-drug bipartite networks before applying the same LOOCV protocol. To this goal, we added artificial transit drug nodes linking existing gene-disease associations (strategy described in Fig. S11). We observed that these artificially added transit nodes increased drastically the performances of the LOOCV (Fig.3 panel B.1). The same phenomenon is observed for the airports multilayer network (Fig.3 panel B.2). In addition, we checked if random perturbations in these artificially enhanced bipartite networks would decrease the performances of the LOOCV. To do so, we progressively randomized the edges in the bipartite networks with artificially increased connectivity until obtaining completely random bipartite networks. We observed that the progressive randomization of the bipartite networks continuously decreased the predictive power of the RWR up to obtaining the same performances as with only two multiplex networks (Fig. S12.A for the airport multiplex networks and S12.B for the biological multilayer networks).

Finally, we repeated all these evaluations using a Link Prediction (LP) protocol (21). In this protocol, we systematically removed gene-disease edges from the gene-disease bipartite network, and predicted the rank of the removed gene using the disease as a seed in the RWR. The LP protocol is applied on the airport multilayer network by removing a French-British edge from the French-British bipartite network, and predicting the rank of the French airport using the British airport node as a seed in the RWR. We overall observed similar behaviors as LOOCV (Fig. S9 and S13).

It is to note that the LOOCV and LP protocols can be used to evaluate the pertinence of adding new multiplex networks in a multilayer network or new network layers in a multiplex network. Both protocols are available within the MultiXrank package.

Parameter space exploration.

We next evaluated the stability of MultiXrank output scores upon variations of the input parameters. We illustrate this exploration of the parameter space with the biological multilayer network composed of two types of nodes: genes and diseases. We first compared the top-5 and top-100 gene and disease nodes prioritized by MultiXrank using 124 different sets of parameters (Fig 4.A, see supplementary section 4.B for the definition of the sets of parameters). We observed that the gene top-ranking is more sensitive to input parameters than the disease top-ranking (Fig 4.A).

To better understand the stability of the output scores upon variations of the input parameters, we proposed a protocol based on 5 successive steps: i) definition of the sets of parameters, ii) construction of a matrix containing the similarities of the RWR output scores obtained with each set of input parameters, using a new similarity measure (equation [17]). We computed these similarities between RWR output scores for each type of node independently (i.e., for genes and diseases).

$$S_{\alpha\beta} = \sum_{j=1}^{m_i} \frac{\sqrt{[(r_{\alpha}^i)_j - (r_{\beta\alpha}^i)_j]^2 + [(r_{\beta}^i)_j - (r_{\alpha\beta}^i)_j]^2}}{\left(\frac{r_{\alpha}^i + r_{\beta}^i}{2}\right)^2} \quad [17]$$

Where α and β define two sets of parameters, m_i is the number of nodes associated with the multiplex network i , r_{α}^i

(resp. r_{β}^i) are the scores associated to the set of parameters α (resp. β) for the multiplex network i , $r_{\alpha\beta}^i$ (resp. $r_{\beta\alpha}^i$) is the distribution of the positions of the nodes associated with the set of parameters α (resp. β) for the distribution associated with β (resp. α), for the multiplex network i .

We next computed a consensus Similarity matrix for each type of node with a normalized euclidean norm of each individual Similarity matrix (equation [18]).

$$S_{\alpha\beta} = \sqrt{\sum_{i=1}^N \frac{(S_{\alpha\beta}^i)^2}{m_i}} \quad [18]$$

Where N is the number of multiplex networks.

The next step, iii) projection of the consensus Similarity matrix into a PCA space, where each dot represents the output scores resulting from a set of parameters (Fig. 4.B). Then, iv) clustering (using k-means on the two first principal components) to identify sub-regions containing similar RWR output scores. Finally, v) comparing the top-ranked nodes obtained with the set of parameters belonging to each cluster (see supplementary section 4.B for details).

We applied this protocol to evaluate the output scores obtained by MultiXrank on the previously defined biological multilayer network composed of the gene multiplex network and the disease monoplex network, using 124 different combinations of parameters. We projected the consensus Similarity matrix into the PCA space and identified 8 clusters (Fig. 4.B). We then focused our analyses on the two clusters defined in the bottom left subspace (clusters number 0 and 5, zoom in Fig. 4.B). The top-100 ranked gene and disease nodes identified using the sets of parameters inside each of the two clusters are overall similar (Fig 4.C). This means that even if the node prioritization can be sensitive to input parameters, we can identify regions of stability on the parameter space. Moreover, the protocol allows identifying the source monoplex/multiplex networks generating the variability in the output scores upon changes in the input parameters.

We applied the protocol to other multilayer networks and observed varied behavior, from highly variable top-rankings and scattered projections in the PCA space for the airport multilayer network (supplementary Fig. S14) to robust top-rankings with well-clustered projections in the PCA space for the biological multilayer network composed of 3 types of nodes (genes, diseases and drugs, supplementary Fig. S15). Overall, our parameter space study reveals different sensitivities to input parameters depending on the multilayer network explored. The protocol is available within the MultiXrank package and can be used to characterize in-depth the sensitivity to input parameters of any multilayer network.

Applications

MultiXrank output scores can be used in a wide variety of applications. Indeed, RWR scores can be employed directly for node prioritization, and they can also be the starting point for clustering (22–24) or embedding (25–27), for instance. We illustrate here the versatility and usefulness of MultiXrank output scores in different use-cases. The first use-case is dedicated to node prioritization in Leukemia using a multilayer biological network composed on two multiplex

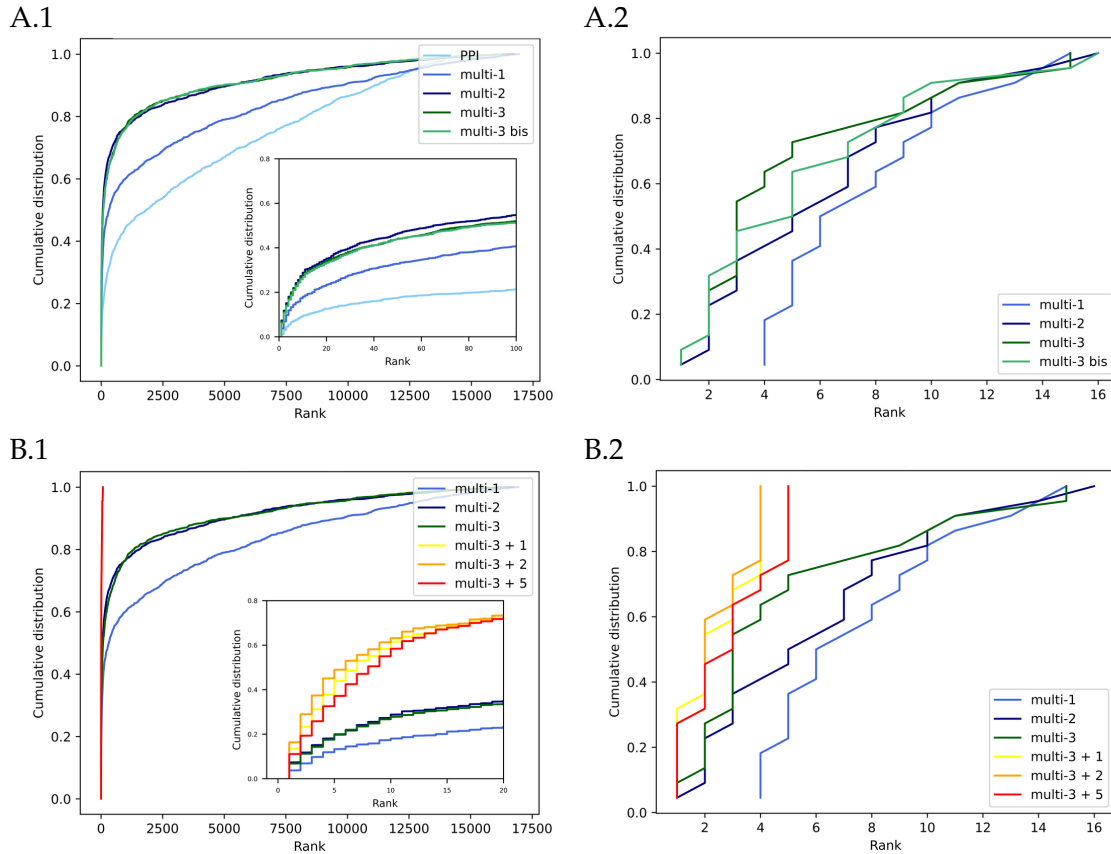


Fig. 3. A.1 and A.2: Cumulative Distribution Functions (CDFs) representing the ranks of the left-out nodes in the LOOCV protocol. A.1: focus on different combinations of biological networks: protein-protein interactions network (PPI), gene multiplex network (multi-1), multilayer network composed of the gene multiplex network and the disease monoplex network (multi-2), and multilayer network composed of the gene multiplex network, the drug multiplex networks and the disease monoplex network for two different sets of parameters (multi-3, multi-3 bis). The multilayer networks are connected by the bipartite networks described in the evaluation section. A.2: focus on different combinations of airports networks: French multiplex network (multi-1), multilayer network composed of the French and British airports multiplex networks (multi-2), and multilayer network composed of the French, British, and German airports multiplex networks for two different sets of parameters (multi-3, multi-3 bis). These multilayer networks are connected by the bipartite networks described in the evaluations section.

B.1-2: Cumulative Distribution Functions (CDFs) representing the ranks of the left-out nodes in the LOOCV protocol for the multi-3 multilayer networks described previously with artificially increased connectivity in the gene-drug and disease-drug bipartite networks thanks to the addition of 1 (multi3+1), 2 (multi3+2) or 5 (multi3+5) transit drug nodes for each gene-disease association (B.1), and with artificially increased connectivity in the French-German and British-German bipartite networks thanks to the addition of 1 (multi3+1), 2 (multi3+2) or 5 (multi3+5) transit German nodes for each French-British airports association (B.2).

networks. We then applied MultiXrank to predict candidate drugs for epilepsy using a large and heterogeneous multilayer network. This second use-case allowed us to compare the results obtained by MultiXrank with an unsupervised approach with the results obtained by Himmelstein et al. with a supervised machine learning approach (3). Finally, in a third use-case, we used MultiXrank output scores to train a supervised classifier to predict gene-disease associations.

Node Prioritization in Leukemia: In order to illustrate the value of MultiXrank for node prioritization, we analyzed two nodes of interest for Leukemia, a well-studied disease for which we can confront our predictions with the knowledge existing in the literature. Our goal is to prioritize nodes around i) Tipifarnib (DB04960), a drug investigated for the treatment of Acute Myeloid Leukemia and other types of cancer (28–30), and ii) HRAS, as mutations in the RAS gene family have been described in a wide variety of tumors, in particular in Myeloid Leukemia (31). The association between these two nodes is particularly relevant as HRAS is

a farnesylated protein and Tipifarnib a farnesyltransferase inhibitor (32). We used HRAS and Tipifarnib as gene and drug seeds, respectively, in MultiXrank applied on a multilayer network composed of a gene multiplex network and a drug multiplex network (supplementary section 3.B for details). A literature survey of the top-10 prioritized genes and drugs demonstrates established or suspected connections with Leukemia (supplementary section 5.A). For instance, the second highest-scoring gene is FNTB, a gene coding the farnesyltransferase and a target of Tripifarnib. Different genes related to signal transduction and known to be relevant for cancer, including RAF1, RASGRP1, RASA1 or ARAF are also identified among the top-scoring genes.

Node Prioritization to predict candidate drugs for epilepsy and comparison of MultiXrank with the Hetionet framework: We applied MultiXrank to prioritize candidate drugs for epilepsy, using as seed the epilepsy disease node (OID:1826) in the large and heterogeneous multilayer network assembled in the Hetionet project (3). This multilayer network is composed

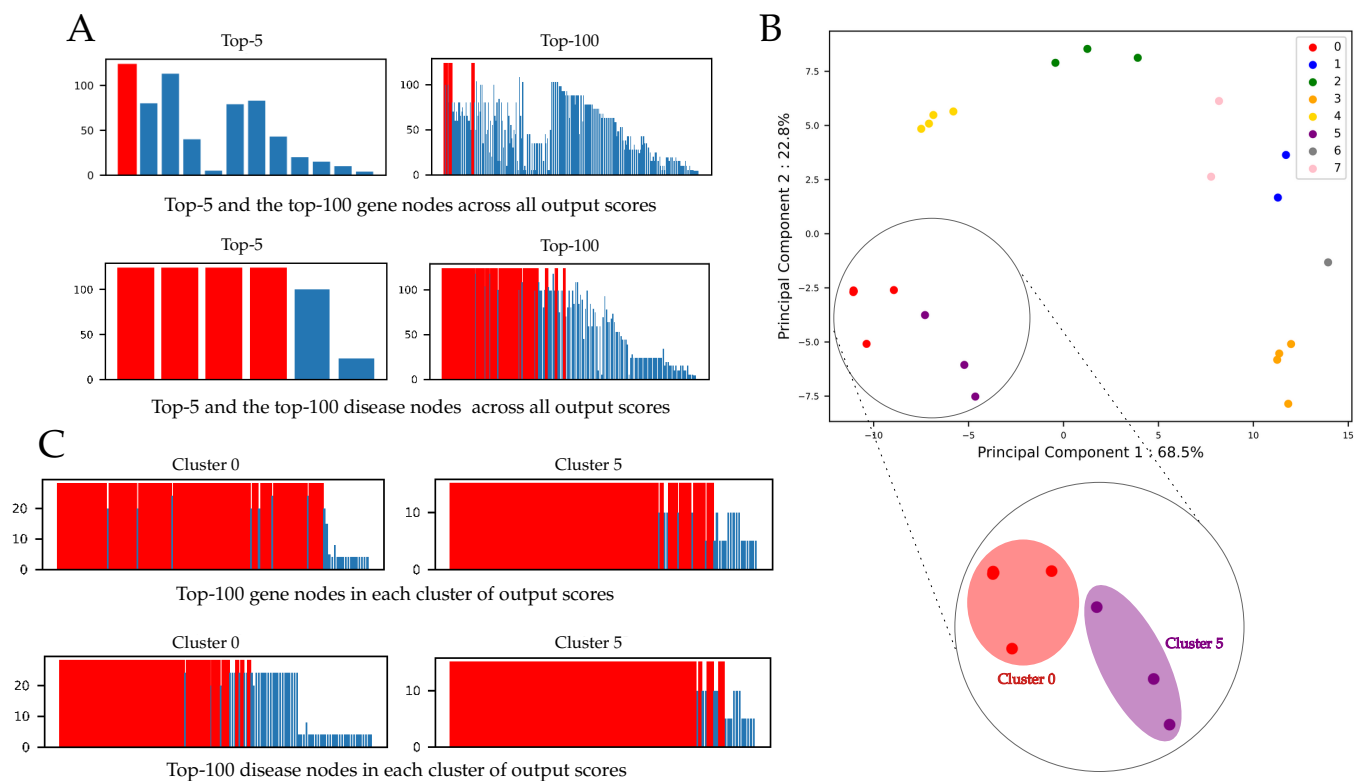


Fig. 4. A: Comparison of the top-5 and top-100 nodes ranked by MultiXrank using a biological multilayer networks composed of the gene multiplex network and the disease monoplex network for different sets of parameters. The top-5 or top-100 ranked nodes for each set of parameters are merged, and the occurrences of each node are counted. The nodes are represented in bars colored in red when the node is found in all top-5 or top-100 scores, and in blue otherwise. B: Clustering in the PCA space of the output scores obtained with MultiXrank on the biological multilayer network composed of a gene multiplex network and a disease monoplex network using different sets of parameters. C: Comparison of the top-100 nodes retrieved for the sets of parameters belonging to clusters 0 and 5 defined in B. The bar is colored in red when a node is found in all top-100 scores, and in blue otherwise.

of nine different types of nodes distributed in multiplex and monoplex networks (supplementary section 3C for details). We compared the drugs top-predicted by MultiXrank (an unsupervised approach) with the drugs top-predicted by the Hetionet approach using a supervised machine learning approach based on regularized logistic regression (3). Many drugs are predicted by both approaches. Indeed, for one of the set of parameters tested in MultiXrank (set of parameters number 4), 59% of the top-100 Hetionet prediction are also in the top-100 of MultiXrank, 80% in the top-200 of MultiXrank, and 99% in the top-500 of MultiXrank (Fig. S18). We checked in detail the 41 drugs retrieved in the top-100 MultiXrank scores that were not identified by the Hetionet approach (supplementary Table S7). We identified different drug classes of interest, including Cytochrome P-450 Substrates, Analgesics and Indoles. A literature survey showed that these three classes of drugs have potential curative effects on epilepsy (33–35). These results indicate that MultiXrank can provide predictions complementary to the Hetionet machine learning approach (for detailed results and statistics, see supplementary section 5.B). In addition, MultiXrank predictions can be easily interpreted thanks to the extraction of the subnetworks underlying the prioritization.

Supervised classification of gene-disease associations: The third use-case is dedicated to the training of a supervised binary random forest classifier to predict new gene-disease

associations. Pertinent predictions of gene-disease associations are crucial for the diagnosis, understanding, and treatment of genetic diseases. Among the approaches available for gene-disease predictions, network-based methods have been particularly employed and demonstrated good performances (36). These network approaches were initially mainly based on unsupervised strategies, but an increasing number of methods are currently testing supervised strategies (36).

We applied MultiXrank (using the parameters described in supplementary Table S8) to two different biological multilayer networks, one composed of the gene multiplex network and the disease monoplex network, and one composed of the gene multiplex network, the drug multiplex network and the disease monoplex network (supplementary section 3.B). In these two multilayer networks, we connected the gene multiplex and the disease monoplex network with a gene-disease bipartite network constructed with an outdated version of DisGeNET (v2.0, 2014 (37)). We then trained binary random forest classifiers with different parameters (38) using the MultiXrank output scores (see supplementary Fig. S19 for the workflow). We tested the performance of the classifiers to predict gene-disease associations that have been added in an updated version of the same bipartite network (DisGeNET v7.0, 2020 (39)). With the first biological multilayer network, the best random forest classifier according to the F1 score had a score equal to 0.90 (supplementary Table S9), which demonstrate that MultiXrank outputs can be used to train a classifier to predict

new gene-disease associations. We observed that the same task using the second biological multilayer network, containing also the drug multiplex networks, show lower performances (F1 score = 0.63, Table S10). These results corroborate our previous observations with the LOOCV and the LP protocols in the evaluations section, i.e. the drug multiplex network does not increase the prediction performances of the RWR.

Discussion

Multilayer networks are nowadays very popular, in particular because they allow to apprehend a larger part of real and engineered systems. In biology, multilayer networks integrating multiscale sources of heterogeneous interactions provide a more comprehensive picture of biological system functionalities. However, data representation as multilayer networks must be accompanied by the development of tools allowing their exploration. Many efforts are thereby dedicated to extend classical network theory algorithms to multilayer systems (4, 40). These algorithms include for instance clustering algorithms (41), Graph Convolutional Networks (42, 43) or meta-path based methods (3, 44). Another important class of network exploration algorithms, such as diffusion kernels or methods based on random walk, is based on the principle of network propagation (40). The methods based on random walk, such as PageRank, biased random walk or Random Walk with Restart (RWR) are widely used in network science. Their versatility indeed allow using the random walk output scores directly for node prioritization and subnetwork extraction, but can also be used as input of downstream analysis pipelines, for instance for supervised classification, clustering or node embedding (27). Different random walk approaches have been adapted to consider multilayered networks. However, many different types of multilayer networks exist, from multiplex to multi-relational, for instance. Network exploration algorithms that have been adapted to handle multilayer networks can often be applied only to specific categories of multilayer networks, such as multiplex networks composed of the same set of nodes.

We propose here MultiXrank, a new tool that proposes an optimized and general formalism for universal RWR on multilayer networks. MultiXrank can be applied to explore multilayer networks composed of any combination of multiplex, monoplex or bipartite networks, and all the layers and edges can be directed and weighted. We complemented MultiXrank with a parameter space exploration protocol to measure the influence of variations in the input parameters on the global stability of the results. It is to note that this parameter space exploration protocol is universal and can be used to study any complex system exploration approach providing scores as outputs.

The output scores of MultiXrank can be used in a wide variety of downstream analyses, such as clustering and embedding. For instance, shallow embedding methods need similarity measure for the optimization of the loss function (27, 45). MultiXrank can produce such a similarity measure respecting the global topology of the network. Using MultiXrank output scores with subsequent embedding would allow taking advantage of the embedding space on the robustness to increase the predictive power of the gene-disease association prediction task(46).

We illustrate the usefulness of MultiXrank with various use-case applications related to biology and human diseases, providing guidelines for users. The MultiXrank package can be applied to any kind of multilayer network such as social, economic, or ecological multilayer networks. MultiXrank is optimized and can handle multilayer networks containing up to millions edges. To consider billion-scale network problems, several strategies can be considered, such as the Block Elimination Approach for RWR (BEAR) that can be exact or approximate (47) or the Best of Preprocessing and Iterative approaches (BEPI) that is an approximate approach (48).

Finally, even if one's initial intuition in data analysis could be that "more data is better", the addition of interaction network layers also brings additional degree of freedom (4). To evaluate the pertinence of the addition of multiplex networks or the addition of layers in a multilayer system, MultiXrank includes a systematic evaluation protocol based on Leave-One-Out-Cross-Validation and Link Prediction. Overall, our results show that adding networks data does not always increase the predictive power of the RWR, as already suggested by previous studies (9). Our evaluation protocol can be used, for the first time to our knowledge, to evaluate in-depth the signal-to-noise of multilayer system combinations.

ACKNOWLEDGMENTS. The project leading to this preprint has received funding from the « Investissements d'Avenir » French Government program managed by the French National Research Agency (ANR-16-CONV-0001), from Excellence Initiative of Aix-Marseille University - A*MIDEX and from the Inserm Cross-Cutting Project GOLD.

- Bianconi G (2018) *Multilayer Networks: Structure and Function*. (Oxford University Press, Oxford), p. 416.
- Duran-Frigola M, et al. (2020) Extending the small-molecule similarity principle to all levels of biology with the chemical checker. *Nature Biotechnology*.
- Himmelstein DS, et al. (2017) Systematic integration of biomedical knowledge prioritizes drugs for repurposing. *eLife* 6:e26726.
- Kivelä M, et al. (2014) Multilayer networks. *Journal of Complex Networks* 2(3):203–271.
- Lee B, Zhang S, Poleksic A, Xie L (2020) Heterogeneous multi-layered network model for omics data integration and analysis. *Frontiers in Genetics* 10:1381.
- Battiston F, Nicosia V, Latora V (2014) Structural measures for multiplex networks. *Phys. Rev. E* 89(3):032804.
- Mucha PJ, Richardson T, Macon K, Porter MA, Onnela JP (2010) Community structure in time-dependent, multiscale, and multiplex networks. *Science* 328(5980):876–878.
- Didier G, Brun C, Baudot A, Gomez S (2015) Identifying communities from multiplex biological networks. *PeerJ* 3:e1525.
- Choobdar S, et al. (2019) Assessment of network module identification across complex diseases. *Nature Methods* 16(9):843–852.
- Li Y, Patra JC (2010) Genome-wide inferring gene-phenotype relationship by walking on the heterogeneous network. *Bioinformatics* 26(9):1219–1224.
- De Domenico M, Solé-Ribalta A, Gómez S, Arenas A (2014) Navigability of interconnected networks under random failures. *Proceedings of the National Academy of Sciences* 111(23):8351–8356.
- Cho H, Berger B, Peng J (2016) Compact integration of multi-network topology for functional analysis of genes. *Cell Systems* 3(6):540–548.e5.
- Valdeolivas A, et al. (2018) Random walk with restart on multiplex and heterogeneous biological networks. *Bioinformatics* 35(3):497–505.
- Lovász L (1993) Random walks on graphs: A survey. *Combinatorics, Paul Erdos is Eighty* 2(1):1–46.
- Brin S, Page L (1998) The anatomy of a large-scale hypertextual web search engine. *Computer Networks and ISDN Systems* 30(1):107–117. Proceedings of the Seventh International World Wide Web Conference.
- Langville AN, Meyer CD (2006) *Google's PageRank and Beyond: The Science of Search Engine Rankings*. (Princeton University Press, USA).
- Pan JY, Yang HJ, Faloutsos C, Duygulu P (2004) Automatic multimedia cross-modal correlation discovery in *Proceedings of the Tenth ACM SIGKDD International Conference on Knowledge Discovery and Data Mining*, KDD '04. (Association for Computing Machinery, New York, NY, USA), p. 653–658.
- Köhler S, Bauer S, Horn D, Robinson PN (2008) Walking the interactome for prioritization of candidate disease genes. *The American Journal of Human Genetics* 82(4):949–958.
- D.Meyer C (2000) Matrix analysis and applied linear algebra. *SIAM*.
- Mordelet F, Vert JP (2011) Prodigy: Prioritization of disease genes with multitask machine learning from positive and unlabeled examples. *BMC Bioinformatics* 12(1):389.
- Zhou M, Zheng C, Xu R (2020) Combining phenotype-driven drug-target interaction prediction

- with patients' electronic health records-based clinical corroboration toward drug discovery. *Bioinformatics* 36:i436–i444.
22. Andersen R, Chung F, Lang K (2007) Using pagerank to locally partition a graph. *Internet Mathematics* 4(1):35–64.
 23. Zhu ZA, Lattanzi S, Mirrokni V (2013) A local algorithm for finding well-connected clusters.
 24. Yi Y, Jin L, Yu H, Luo H, Cheng F (2021) Density sensitive random walk for local community detection. *IEEE Access* 9:27773–27782.
 25. Liu Z, Huang C, Yu Y, Fan B, Dong J (2020) Fast attributed multiplex heterogeneous network embedding in *Proceedings of the 29th ACM International Conference on Information & Knowledge Management, CIKM '20*. (Association for Computing Machinery, New York, NY, USA), p. 995–1004.
 26. Dursun C, Smith JR, Hayman G, Kwitek AE, Bozdogan S (2020) Neco: A node embedding algorithm for multiplex heterogeneous networks in *2020 IEEE International Conference on Bioinformatics and Biomedicine (BIBM)*. (IEEE Computer Society, Los Alamitos, CA, USA), pp. 146–149.
 27. Pio-Lopez L, Valdeolivas A, Tichit L, Remy E, Baudot A (2021) Multiverse: a multiplex and multiplex-heterogeneous network embedding approach. *Scientific Reports* 11(1):8794.
 28. Thomas X, Elhamri M (2007) Tipifarnib in the treatment of acute myeloid leukemia. *Biologics : targets & therapy* 1(19707311):415–424.
 29. Yanamandra N, et al. (2011) Tipifarnib-induced apoptosis in acute myeloid leukemia and multiple myeloma cells depends on ca2+ influx through plasma membrane ca2+ channels. *J Pharmacol Exp Ther* 337(3):636.
 30. Luger S, et al. (2015) Tipifarnib as maintenance therapy in acute myeloid leukemia (aml) improves survival in a subgroup of patients with high risk disease. results of the phase iii intergroup trial e2902. *Blood* 126(23):1308–1308.
 31. Tyner JW, et al. (2009) High-throughput sequencing screen reveals novel, transforming ras mutations in myeloid leukemia patients. *Blood* 113(19075190):1749–1755.
 32. McGeedy P, Kuroda S, Shimizu K, Takai Y, Gelb MH (1995) The farnesyl group of h-ras facilitates the activation of a soluble upstream activator of mitogen-activated protein kinase. *The Journal of biological chemistry* 270(44):26347–51.
 33. Runtz L, et al. (2018) Hepatic and hippocampal cytochrome p450 enzyme overexpression during spontaneous recurrent seizures. *Epilepsia* 59(1):123–134.
 34. Tomić M, Peckoza U, Micov A, Vučković S, Stepanović-Petrović R (2018) Antiepileptic drugs as analgesics/adjuvants in inflammatory pain: current preclinical evidence. *Pharmacology & therapeutics* 192:42–64.
 35. Swathi K, Sarangapani M (2017) Evaluation of anti-epileptic effect of new indole derivatives by estimation of biogenic amines concentrations in rat brain. *Advances in experimental medicine and biology* 988:39–48.
 36. Ata SK, et al. (2020) Recent advances in network-based methods for disease gene prediction. *Briefings in bioinformatics*.
 37. Piñero J, et al. (2015) Disgenet: a discovery platform for the dynamical exploration of human diseases and their genes. *Database (Oxford)* 2015(bav028).
 38. Liu H, et al. (2019) Predicting effective drug combinations using gradient tree boosting based on features extracted from drug-protein heterogeneous network. *BMC Bioinformatics* 20(1):645.
 39. Piñero J, et al. (2020) The disgenet knowledge platform for disease genomics: 2019 update. *Nucleic Acids Res* 48(D1):D845–D855.
 40. Boccaletti S, et al. (2014) The structure and dynamics of multilayer networks. *Physics Reports* 544(1):1–122.
 41. Huang X, Chen D, Ren T, Wang D (2021) A survey of community detection methods in multi-layer networks. *Data Mining and Knowledge Discovery* 35(1):1–45.
 42. Ghorbani M, Baghshah MS, Rabiee HR (2019) Mgn. *Proceedings of the 2019 IEEE/ACM International Conference on Advances in Social Networks Analysis and Mining*.
 43. Shanthamallu US, Thiagarajan JJ, Song H, Spanias A (2020) Gramme: Semisupervised learning using multilayered graph attention models. *IEEE Transactions on Neural Networks and Learning Systems* 31(10):3977–3988.
 44. Zhang X, Zou Q, Rodríguez-Patón A, ZENG X (2019) Meta-path methods for prioritizing candidate disease mirnas. *IEEE/ACM Transactions on Computational Biology and Bioinformatics* 16(1):283–291.
 45. Hamilton WL, Ying R, Leskovec J (2018) Representation learning on graphs: Methods and applications.
 46. Nelson W, et al. (2019) To embed or not: Network embedding as a paradigm in computational biology. *Frontiers in genetics* 10(31118945):381–381.
 47. Shin K, Jung J, Lee S, Kang U (2015) Bear: Block elimination approach for random walk with restart on large graphs in *Proceedings of the 2015 ACM SIGMOD International Conference on Management of Data, SIGMOD '15*. (Association for Computing Machinery, New York, NY, USA), p. 1571–1585.
 48. Jung J, Park N, Lee S, Kang U (2017) Bepi: Fast and memory-efficient method for billion-scale random walk with restart in *Proceedings of the 2017 ACM International Conference on Management of Data, SIGMOD '17*. (Association for Computing Machinery, New York, NY, USA), p. 789–804.